Original Article

HEALTH SCIENCES
MEDICINE

DOI: 10.32322/jhsm.1100231
J Health Sci Med 2022; 5(4): 1151-1155

The comparison of chest X-ray and CT visibility according to size and lesion types in the patients with COVID-19

Emrah Doğan[1], Canan Gürsoy[2], Özge Oral Tapan[3], Cenk Elibol[4], Turhan Togan[5], Sema Demirbilek[6]

[1]Mugla Sıtkı Kocman University, Faculty of Medicine, Radiology, Muğla, Turkey
[2]Mugla Sıtkı Kocman University Education and Research Hospital, Anaesthesiology and reanimation, Muğla, Turkey
[3]Mugla Sıtkı Kocman University, Faculty of Medicine, Pulmonology, Muğla, Turkey
[4]Muğla Training and Research Hospital, Department of Radiology, Muğla, Turkey
[5]Mugla Sıtkı Kocman University, Faculty of Medicine, Infectious Diseases, Muğla, Turkey
[6]Mugla Sıtkı Kocman University, Faculty of Medicine, Anaesthesiology and reanimation, Muğla, Turkey

Cite this article as: Doğan E, Gürsoy C, Oral Tapan Ö, Elibol C, Togan T, Demirbilek S. The comparison of chest X-ray and CT visibility according to size and lesion types in the patients with COVID-19. J Health Sci Med 2022; 5(4): 1151-1155.

ABSTRACT

Introduction: Chest X-ray (CXR) is one of the routinely used radiological examinations in COVID-19. However, the lesion detectability level of CXR is low. To date, to the best of our knowledge, the visualization quality of X-ray in COVID-19 has not been specifically evaluated in different lesions. Our study aims to determine the visualization quality of CXR in COVID-19 patients according to elementary lesions.

Material and Method: 52 COVID-positive patients (26 Males and 26 Females); 69,6346±15,14250 (32-89) years [mean±SD age (range)] were included in the study. 98 different elementary lesions of lung detected on CT were evaluated in six different groups (consolidation, indeterminate ground-glass opacity (IGGO), dense GGO (DGGO), reversed halo, parenchymal band and curvilinear band). Lesions were compared with CXR taken on the same day. The detectability rates of the lesions on CXR were evaluated.

Results: The mean sizes of CXR negative and CXR positive lesions for every group (consolidations, IGGO, DGGO, reversed halo sign, parenchymal band, curvilinear band) were respectively 1.36 cm -5.75 cm, 3.44 cm -5.50 cm, 2.25 cm -5.06 cm, 2.5cm -4.09 cm, N/A -3.14 cm and 1 cm -4.5 cm. According to Mann-Whitney U analysis, p values were found as (respectively in consolidations, IGGO, DGGO, reversed halo sign, and curvilinear band) 0.0001p, 0.145, 0.0001 p, 0.143 and 0.286. Given consolidation and DGGO groups, there was a statistically significant difference between non-visualized and visualized groups. According to ROC analysis, cut-off values were respectively 3 cm and 3.5 cm for consolidation and DGGO.

Conclusion: Our study showed that consolidations smaller than 3 cm and DGGO smaller than 3.5 cm are difficult to visualize with CXR. Although there is no definite cut-off value in other elementary lesions, the visualization ratio of parenchymal bands and curvilinear bants on chest X-rays is quite high. IGGOs may not be detected even at higher dimensions. Reversed halos less than 3 cm can rarely be detected on CXR.

Keywords: COVID-19, Chest X-Ray, computed tomography, thorax radiology

INTRODUCTION

A novel highly contagious respiratory pathogen in the corona virus (CV) group was first reported in December 2019 in Wuhan, China. This virus is named severe acute respiratory syndrome coronavirus-2-(SARS-coV-2) and the disease of this virus was called officially COVID-19 by World Health Organization (1-3). The first official case was reported in March 2020 in Turkey (4).

COVID-19 is a disease that may be led to various levels of pneumonia, necrotizing encephalopathy, systemic and pulmonary thromboembolism, acute respiratory distress syndrome, respiratory failure, systemic inflammatory response and sepsis. Chest computed tomography (CT) is a key diagnostic method coupled with Polymerase Chain Reaction (PCR) as the primary evaluation and follow-up method in COVID-19 (5,6). CT can show the progression of the disease, its severity, and the effectiveness of the treatment. Especially in the early phase, when the viral load is low, CT can be

Corresponding Author: Emrah Doğan, dr_e_dogan@hotmail.com
Received: 07.04.2022 **Accepted:** 27.06.2022

This work is licensed under a Creative Commons Attribution 4.0 International License.

positive (7). CT was used as a screening test almost as widely as PCR in our country at the beginning of the pandemic (8). However, the use of CT decreased with the increase in experience about the disease in the forthcoming days and clinical findings and the use of Chest X-rays (CXR) became more prominent (9,10). The effectiveness of CRX in detecting COVID-19's radiological findings is quite low compared to CT. So far, many studies have been conducted on the use of CRX in patients with COVID-19 (11,12). However, to the best of our knowledge, there is no lesion-specific study on this subject in the literature. In addition, there is also no study on the lesions that can be detected over which cut-off value. Our study is the first study with these aspects. In this paper, the detection rates of elementary lesions due to COVID-19 with CRX are discussed. Our study aims to determine the visualization quality of CXR according to elementary lesions in COVID-19.

MATERIAL AND METHOD

Study Design and Patient Population

Our retrospective study was approved by Muğla Sıtkı Koçman University Human Research Ethics Committee (Date: 04.06.2020, Decision No: 200140). The Republic of Turkey Ministry of Health Scientific Research Council approved this study before applying to the ethics committee. Also, the pandemic board approved to study. All procedures were performed adhered to the ethical rules and principles of the Helsinki Declaration.

52 patients with both PCR and CT positivity and having CXR (26 Males and 26 Females); 69,6346±15,14250 (32-89) years [mean± SD age, (range)] were included in the study. All of the patients' CT findings were also compatible with COVID-19 pneumonia [In the typical group according to Radiological society of North America (RSNA) classification].

Real-time PCR (RT-PCR Charite, Berlin, Germany) test was performed from the nasopharyngeal and oropharyngeal swabs obtained at a time interval of 24 hours. Two consecutive negative RT-PCR results were considered negative. The demographic characteristics, clinical findings, and laboratory results of the patients were collected from PACS and hospital data systems.

CT Technique

All CT scans were performed without the contrast agent, during deep inspiration, and in the supine position. CT images were obtained using a 256-slice multi-detector CT scanner (Somatom, Siemens Healthcare, Erlangen, Germany) or 4 slices of Toshiba-TCT-60 AX (Toshiba Medical system Corporation, Yokohama, Japan) devices. The following technical parameters were used; tube voltage, 100–120 kV; tube current–exposure time product, 200–300 mAs; pitch, 0.9125-1.375 and; and section thickness after reconstruction, 1-1.25 mm. The room was decontaminated with 62-71% ethanol or 0.1% sodium hypochlorite. Passive air exchange was applied for 40-60 minutes after the thorax CT examination.

CT image analysis: Two experienced radiologists evaluated CT images that belong to patients who were diagnosed to be COVID-19. The patients were re-evaluated together in case of discrepancy. The incidence of o lung elementary patterns seen on CT images was determined. The radiological features of GGO, consolidation, reversed halo sign, parenchymal band and the curvilinear band were evaluated.

CXR technique: All CXRs were taken using digital radiographs with DRGEM TOPAZ 100 ma X-ray machine. In accordance with the hospital isolation protocol, CXRs were taken in the anteroposterior (AP) plane for bed-ridden patients whereas in the posteroanterior (PA) plane for proper patients. Follow-up CXRs were obtained according to the same protocol.

CXR analysis: The visibility of the lesions detected on CT was evaluated by comparing the CT Scenogram separately for each lesion.

Statistical Analysis

All continuous variables were expressed as medians, intervals, counts, and percentages. The data were recorded (Excel 2010, Microsoft) and analysed using statistical software (SPSS, version 22.0, IBM). Continuous variables were expressed as mean±SD (Standard deviation) values. CT findings were compared with Mann Whitney-U test because the groups were inhomogeneous and independent. $P < 0.05$ values were considered statistically significant. Cut off values were determined with ROC analysis.

RESULTS

Six different elementary lung lesions in 52 patients (26 males, 26 females) were probed. Lesions in the form of consolidation, GGO, reversed halo sign, curvilinear and parenchymal bands were evaluated in CT. The mean sizes of consolidation, indeterminate GGO(IGGO) and dense GGO(DGGO) were altered in the range from 3.68 to 4.48 cm. Parenchymal and curvilinear bands' thicknesses were ranged from 0.31 to 0.58 mm. The number of lesions, minimum and maximum dimensions, mean values and standard deviation values are as follows (**Table 1**).

Table 1. Table shows the number of the elementary lesions, minimum sizes (cm), maximum sizes (cm), mean values (cm) and standard deviation (cm) of the lesions.

	N	Min	Max	Mean	Std. Deviation
Consolidation	38	1.00	13.00	4.4868	2.85810
IGGO	11	2.00	10.00	3.8182	2.43180
DGGO	26	1.00	10.00	3.9808	2.05173
Reversed Halo	8	2.00	6.00	3.6875	1.33463
Parenchymal B	8	0.400	0.800	0.57500	0.158114
Curvilinear B	7	0.200	0.400	0.31429	0.069007

Visualization rates of CRX were evaluated. While the visualization rates of fibrotic bands (in parenchymal band 100%, in curvilinear band 85.7%) are highest, reversed halo sign and consolidation are highly visualized with 75% and 71.1% ratios, respectively. DGGOs were detectable in 61.5% of the patients, while IGGOs were only detected in 18.2%. Detailed visualization rates of elementary lesions in CXR are as follows (**Table 2**).

Visible and non-visible groups were compared as two inhomogeneous independent groups with Mann Whitney-U and Wilcoxon Z tests. Out of consolidation and DGGO, there is a statistically significant difference between the visible and non-visible groups, which differs significantly in size ($p<0.05$). There was no significant difference in the findings of IGGO, reversed halo sign and curvilinear band. For this reason, although an exact cut-off value can be determined in terms of visibility value for these three findings, a definite value cannot be mentioned. Test values, Z values and two tailed and single tailed P values are given in the table (**Table 3**).

Test Statistics[a]

A cut-off value was determined by ROC test for elementary lesions with significant differences between values. According to ROC analysis; cut-off value was 3 cm for DGGOs whereas 3.5 cm for consolidations.

DISCUSSION

PCR test is accepted as the gold standard in the diagnosis of COVID-19 (13). However, radiological evaluations are frequently used for rapid diagnosis. It is recommended that CT should be preferred primarily in cases where there is clinical and PCR incompatibility, as well as in the presence of embolism, malignancy, and severe respiratory distress (14,10). CXR is the first preferred examination in the radiological algorithm. However, the false negativity of CXR is quite high. While the sensitivity and specificity of CT is 98-99%, in CXR this rate remains at 63% (The rates alter between 60% and 90%) (10). To date, many studies have been conducted to determine the specificity and sensitivity of CXR (10,12,15,16). However, to the best of our knowledge, there is no study on which lesions CXR is ineffective in diagnosis and in which size lesions it is more helpful.

Typical radiological presentation of COVID-19 pneumonia is characterized by consolidation and GGO involving the peripheral, basal, and posterior parts of lung (17). The prevalence of GGO and consolidation has been reported between 46% and 100% in previous studies (7). The term GGO refers to increased CT attenuation with preserving bronchial and vascular markings. GGO had different radiological characters in mild and prominent forms. Therefore, in our study, these two findings were called and evaluated as different entities as IGGO and DGGO (18, 19).

Table 2. Table shows visible and non-visible elementary lesions' number and percentage according to six different group. Abbreviations; RH: Reversed halo sign PB: Parenchymal band CLB: Curvilinear band

Elementary lesions	Consolidation Freq (N)	Consolidation Per (%)	IGGO Freq (N)	IGGO Per (%)	DGGO Freq(N)	DGGO Per (%)
Non-visible	11	28.9	9	81.8	10	38.5
Visible	27	71.1	2	18.2	16	61.5
Total	38	100.0	11	100.0	26	100.0
Elementary lesions	**RH Freq(N)**	**RH Per (%)**	**PB Freq (N)**	**PB Per (%)**	**CLB Freq (N)**	**CLB Per (%)**
Non-visible	2	25.0	0	0.00	1	14.3
Visible	6	75.0	8	100.0	6	85.7
Total	8	100.0	8	100.0	7	100.0

Table 3. The table shows statistical between analysis visible and nonvisible groups in the five different group. We didn't make a comparison for parenchymal band because there was no non-visible lesion in the sample group.

	Consolidation	IGGO	DGGO	Reversed Halo	CLB
Mann-Whitney U	.000	2.000	7.500	1.500	.000
Wilcoxon W	66.000	47.000	62.500	4.500	1.000
Z	-4.814	-1.673	-3.857	-1.518	-1.673
Asymp. Sig. (2-tailed)	0.0001	0.094	0.0001	0.129	0.094
Exact Sig. (2*(1-tailed Sig.))	0.0001	0.145	0.0001	0.143	0.286

a. Grouping Variable: visible-non visible ; Consolidation, IGGO, DGGO, reversed Halo, CLB, b. Not corrected for ties.

GGO without consolidation is a radiological finding that is seen mostly in the early stages of the COVID-19 (18). It often accompanies consolidations. The visibility of GGO is more difficult than consolidation since HU values and density of GGO are lower than in consolidation. If we sort the lesions according to density, the line is consolidation > DGGO > IGGO, respectively (20,21). According to the results of our study, DGGO over 3.5 cm and consolidations over 3 cm can be easily detected with CXR. The visualization rate in consolidation was 71.1%, whereas in DGGO was 61.5%. It is not possible to talk about such a size limit for IGGO. Considering the detection rate in CXR, no statistically significant difference was found between the groups when patients with and without IGGO were compared. Even, some IGGOs with gross sizes up to 10 cm could not be visualized with CXR in our study. The visualization rate was BGGO is quite low with 18.2%.

The reversed halo sign was a disease-specific finding normally used in the diagnosis of organizing pneumonia

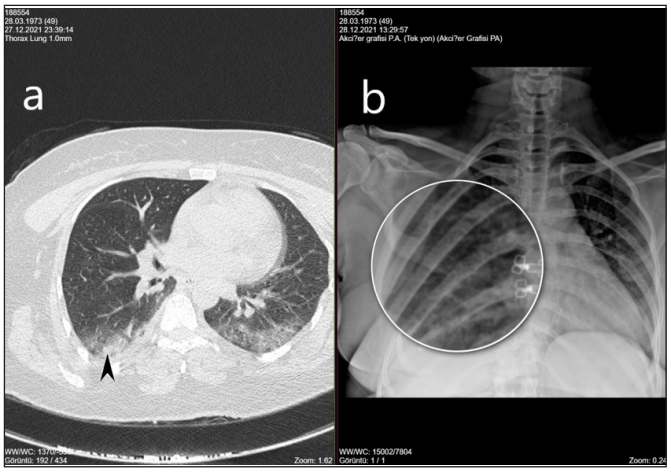

Figure 1a. In the CT sections passing through the inferior pulmonary vein level in the axial sections, the consolidation area with an anteroposterior thickness of 2 cm (cutted arrowhead) accompanied by GGO 1b. This consolidation is not seen in the magnified CRX image taken from the same area

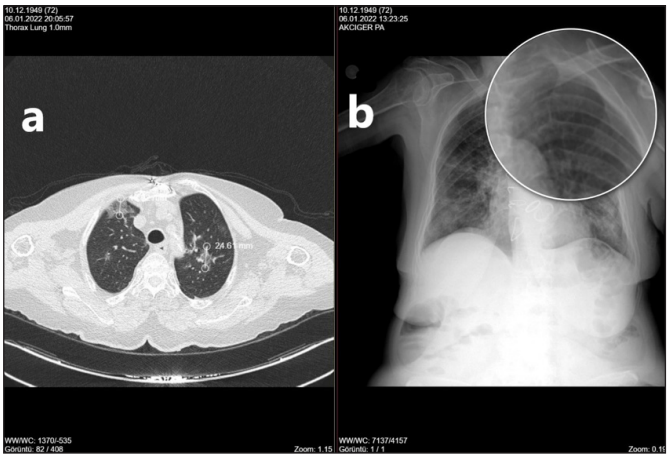

Figure 2a. A DGGO is present in the upper left quadrant. 2b. No lesion was detected in the same area on CRX.

(22). However, after the COVID-19 pandemic, it has been included in the literature in a different way as a radiological finding accompanying the novel disease with a high rate (23). Reversed halo's prevalence varies between 1.7% -15.1% (6). Therefore, the finding was added to the study. According to the results of our study, Reversed halo sign is visualized with CRX at a rate of 75%. A cut off value was not found with the ROC test. The size of the central clear area and the density of the peripheral ring (as consolidation, DGGO or IGGO) were thought to be effective in the visualisation. Notwithstanding, we can say that the detection rate of reversed halos over 3 cm is quite high.

In the late stages of COVID-19, however, parenchymal changes and curvilinear bands overlapping with old filtration areas are quite common (6). In our study, these findings were also evaluated. Parenchymal bands may occur late in the disease secondary to true fibrosis or sub-segmental bronchial plugs. Curvilinear bands are common in the late-covid and post-covid periods, especially in the posterior and basal areas where COVID-19 is more affected (24,25). The thickness of this band is measured in mm, unlike other lesions. Although the dimensions are small, their visibility is quite high compared to others. According to the results of our study, parenchymal bands could be detected at a rate of 100% and curvilinear bands at a rate of 85.7% with CRX.

Our results show that it is seen that the mean lesion size ranges between 3.68 and 4.48 cm for consolidation, GGO, and RHS. Considering that the mean visualization limit is 3-3.5 cm, it is seen that the majority of the lesions in the COVID-19 are visualized lesions. In this respect, the findings of our study support the previous study findings showing the sensitivity values of CRX at least 60%. However, considering that approximately 40% of the lesions are below 3 cm, visualization rates of up to 90% stated in some studies are too optimistic (10).

There are some limitations of our study. CTs and CXRs taken on the same day were compared, ignoring hourly differences. However, the reflection of this hourly clinical change on the radiological change is minimal. In addition, the number of patients is limited, since CRX and CT were not taken simultaneously in each patient at the desired time interval and the study was a single-center study. However, according to the G power test (51 patients), it is above sufficient sample sizes. In addition, hidden areas were not taken into account in the study. Only the visualization rate of localized lesions at the point that can be seen on both CRX and CT was evaluated. Lung tissue is not of the same thickness in the apical area and basally, and the magnification of the lesions located anteriorly and posteriorly is different. However, the effect of these technical physics rules on the routine is quite low.

CONCLUSION

In COVID-19 pneumonia, CXR can mostly detect curvilinear bands and parenchymal bands and DGGO, reversed halo sign and consolidations as long as greater than 3-3.5 cm. According to the results of our study, approximately 60% of COVID-19 lesions are over 3 cm. Therefore, CXR can detect most of the Covid lesions. The usefulness of CRX in detecting IGGO is greatly limited with %18,2 visualisation rate. Although CXR positive findings support the diagnosis, negative findings do not exclude the presence of a lesion.

ETHICAL DECLARATIONS

Ethics Committee Approval: The study was initiated with the approval of the Muğla Sıtkı Koçman University Human Researches Ethics Committee (Date: 04/06/2020, Decision No: 200140).

Informed Consent: Because the study was designed retrospectively, no written informed consent form was obtained from patients.

Referee Evaluation Process: Externally peer-reviewed.

Conflict of Interest Statement: The authors have no conflicts of interest to declare.

Financial Disclosure: The authors declared that this study has received no financial support.

Author Contributions: All of the authors declare that they have all participated in the design, execution, and analysis of the paper, and that they have approved the final version.

REFERENCES

1. Sayar M S, Bulut D, Çelik S, Burulday V, Sarikaya R, Kurt N. The impact and relationship of inflammatory markers and radiologic involvement in the COVID-19 patients. J Health Sci Med 2021; 4: 416-21.
2. Doğan E, Tapan U, Tapan ÖO, Alaşan F, Olcay SS, Olcay TÇ. A case of B. 1.1. 7 SARS-CoV-2 UK strain with an atypical radiological presentation. Monaldi Arch Chest Dis 2021; 91: 1840.
3. Doğan E, Olcay SS, Olcay TÇ, Tapan U, Tapan OO, Alaşan F. A case of post-COVID-19 fibrosis mimicking Thoracic Manifestation of Ankylosing Spondylitis. Acta Medica Lituanica 2022; 29: 10.
4. Gürsoy C, Tapan ÖO, Dogan E, Togan T, Demirbilek SG. COVID-19 Pneumonia during Hydroxychloroquine Treatment of Rheumatoid Arthritis. J Coll Physicians Surg Pak 2020;30:168-170.
5. Ayyıldız A, Çobaner N, Yelken B. Sepsis induced coagulopathy score and D-dimer levels in COVID-19 patients followed in intensive care; what has changed in COVID era? J Health Sci Med 2022; 5: 94-8.
6. Ufuk F, Savaş R. Chest CT features of the novel coronavirus disease (COVID-19). Turk J Med Sci 2020; 50: 664-78.
7. Tenda ED, Yulianti M, Asaf MM, et al. The importance of chest CT scan in COVID-19. Acta MedIndones 2020; 52: 68-73.
8. Mutlu P, Mirici A, Gönlügür U, et al. Evaluating the clinical, radiological, microbiological, biochemical parameters and the treatment response in COVID-19 pneumonia. J Health Sci Med 2022; 5: 544-51.
9. Öztürk Durmaz Ş, Sümer Coşkun A, Yalçın AN. Clinical and prognostic evaluation of patients admitted to the COVID-19 pandemic unit of the emergency department. J Health Sci Med 2021; 4: 835-9.
10. Sathi S, Tiwari R, Verma S, et al. Role of chest X-Ray in coronavirus disease and correlation of radiological features with clinical outcomes in Indian patients. Can J Infect Dis Med Microbiol 2021; 2021: 6326947.
11. Yasin R, Gouda W. Chest X-ray findings monitoring COVID-19 disease course and severity. The Egyptian J Radiol Nuclear Med 2020; 51: 193.
12. Ulgen A, Çetin Ş, Balcı P, et al. COVID-19 outpatients and surviving inpatients exhibit comparable blood test results that are distinct from non-surviving inpatients. J Health Sci Med 2021; 4: 306-313.
13. Durmuş E, Guner NG, Güneysu F, Aslan N, Yurumez Y. Review of COVID-19 vaccinated patients' emergency room admissions. J Health Sci Med 2022; 5: 18-21.
14. Özdemirel ŞT, Akkurt ES, Ertan Ö, Gökler ME, Özyürek BA. Complications with moderate-to-severe COVID-19 during hospital admissions in patients with pneumonia. J Health Sci Med 2021; 4: 766-71.
15. Martínez Chamorro E, Díez Tascón A, Ibáñez Sanz L, Ossaba Vélez S, Borruel Nacenta S. Radiologic diagnosis of patients with COVID-19. Radiologia (Engl Ed) 2021; 63: 56-73.
16. Nava-Muñoz Á, Gómez-Peña S, Fuentes-Ferrer ME, et al. COVID-19 pneumonia: relationship between initial chest X-rays and laboratory findings. Radiologia 2021; 63: 484-94.
17. Akçay MŞ, Özlü T, Yılmaz A. Radiological approaches to COVID-19 pneumonia. Turk J Med Sci 2020; 50: 604-10.
18. Cozzi D, Cavigli E, Moroni C, et al. Ground-glass opacity (GGO): a review of the differential diagnosis in the era of COVID-19. Jpn J Radiol 2021; 39: 721-32.
19. Han X, Fan Y, Alwalid O, et al. Six-month follow-up chest CT findings after severe COVID-19 pneumonia. Radiology 2021; 299: 177-86.
20. Mehrabi S, Fontana S, Mambrin F, et al. Pitfalls of computed tomography in the coronavirus 2019 (COVID-19) era: a new perspective on ground-glass opacities. Cureus 2020; 12: e8151.
21. Parekh M, Donuru A, Balasubramanya R, Kapur S. Review of the cChest CT differential diagnosis of ground-glass opacities in the COVID era. Radiology 2020; 297: E289-E302.
22. Dogan E, Tapan U, Tapan, OO, Togan T, Çelik ÖI. Idiopathic focal organizing pneumonia mimicking malignancy. Pan African Med J 2020; 36: 1-7
23. Gürbüz D, Tunç MK, Yıldız H, Kalkan A, Yıldırmak MT, Önder H. "Reversed Halo" sign on chest computed tomography in COVID-19 pneumonia. Eur Arch Med Res 2021: 261-7.
24. Samir A, Elabd AM, Mohamed W, Baess AI, Sweed RA, Abdelgawad MS. COVID-19 in Egypt after a year: the first and second pandemic waves from the radiological point of view; multi-center comparative study on 2000 patients. Egyptian J Radiol Nuclear Med 2021; 52: 1-13.
25. Vijayakumar B, Tonkin J, Devaraj A, et al. CT Lung abnormalities after COVID-19 at 3 months and 1 year after hospital discharge. Radiology 2021; 211746.